

Supporting information

Theoretical and Experimental Insights into Applicability of Solid-State ^{93}Nb NMR in Catalysis

Evgeniy PAPULOVSKIY^{1,2}, Alexandre A. SHUBIN^{1,2}, Victor V. TERSKIKH³, Christopher
PICKARD^{4,*} and Olga B. LAPINA^{1,2,*}

¹ Boreskov Institute of Catalysis, 630090 Novosibirsk, Russia

² Novosibirsk State University, 630090 Novosibirsk, Russia

³ Emerging Technologies Division, National Research Council Canada, Ottawa, Ontario,
Canada K1A 0R6

⁴ University College London, London, United Kingdom WC1E 6BT

* corresponding authors:

Christopher Pickard, University College London, London, United Kingdom WC1E 6BT, c.pickard@ucl.ac.uk
Olga B. LAPINA, Boreskov Institute of Catalysis, Novosibirsk, Russia 630090, phone: +73833269505, fax: +7
3833 30 80 56, olga@catalysis.ru

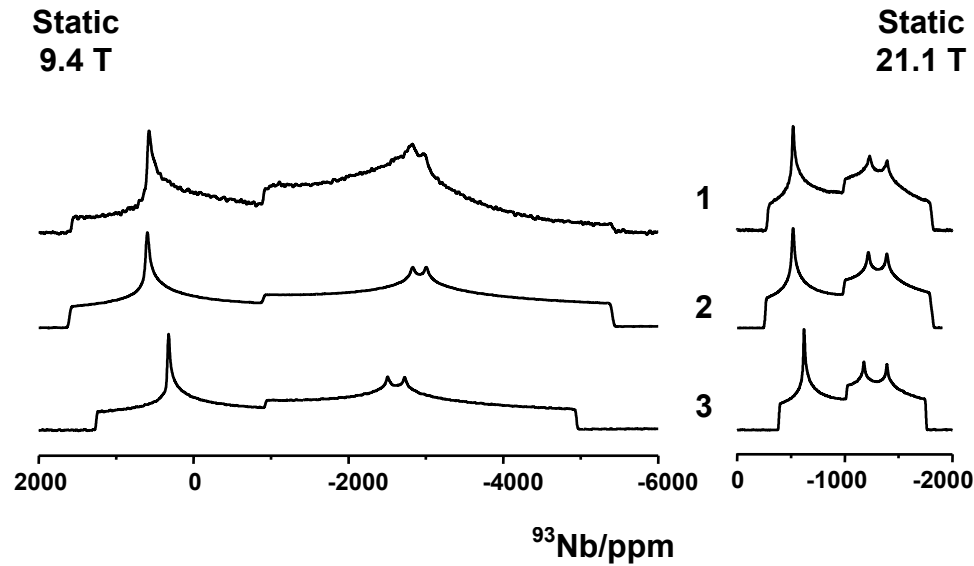


Figure S1. ^{93}Nb NMR spectra of a stationary powdered sample of YNbO_4 acquired at 9.4 T (left) and at 21.1 T (right). (1) Experimental spectra, (2) Simulated spectra with NMR parameters determined in [1] from the experimental spectra, $\delta_{\text{iso}} = -845$ ppm, $\delta_{\delta} = -200$ ppm, $\eta_{\delta} = 0.480$, $C_Q = 82.00$ MHz, $\eta_Q = 0.38$, $\alpha, \beta, \gamma = 15, 16, 80$, (3) Simulated spectra with NMR parameters obtained via GIPAW calculations, $\delta_{\text{iso}} = -901$ ppm, $\delta_{\delta} = -191$ ppm, $\eta_{\delta} = 0.515$, $C_Q = 76.4$ MHz, $\eta_Q = 0.41$, $\alpha, \beta, \gamma = 180, 21, 90$.

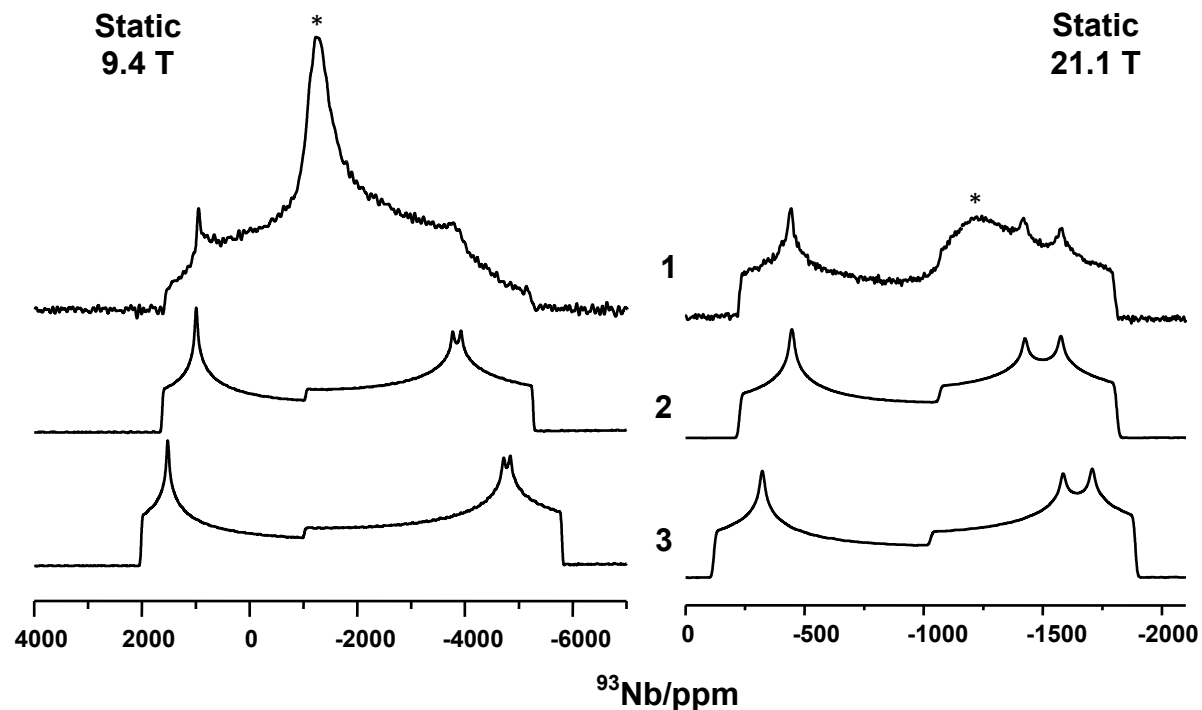


Figure S2. ^{93}Nb NMR spectra of a stationary powdered sample of LaNbO_4 acquired at 9.4 T (left) and at 21.1 T (right). **(1)** Experimental spectra. **(2)** Simulated spectra with NMR parameters determined in [2] from the experimental spectra, $\delta_{\text{iso}} = -853$ ppm, $\delta_{\delta} = -238$ ppm, $\eta_{\delta} = 0.559$, $C_Q = 86.55$ MHz, $\eta_Q = 0.19$, $\alpha, \beta, \gamma = 13, 11, 85$. **(3)** Simulated spectra with NMR parameters obtained via GIPAW calculations, $\delta_{\text{iso}} = -818$ ppm, $\delta_{\delta} = -225$ ppm, $\eta_{\delta} = 0.625$, $C_Q = 95.30$ MHz, $\eta_Q = 0.11$, $\alpha, \beta, \gamma = 0, 9, 90$. (*) indicates an impurity.

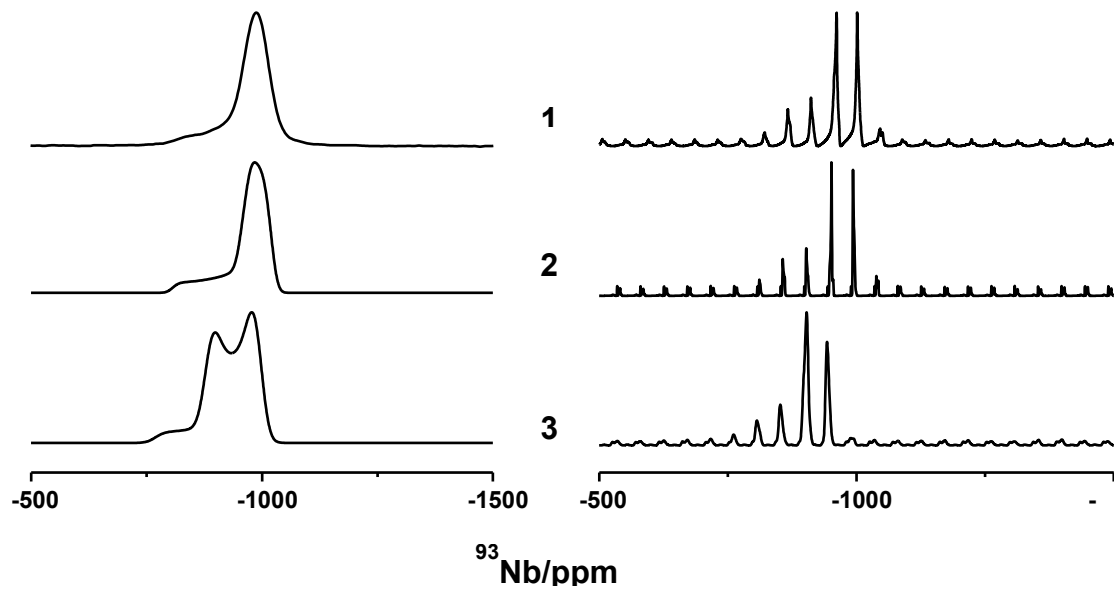


Figure S3. ${}^{93}\text{Nb}$ NMR spectra of a stationary powdered sample of Li_3NbO_4 acquired at 9.4 T. (1) Experimental spectrum. (2) Simulated spectrum using experimental NMR parameters determined in [1] from the experimental spectra, $\delta_{\text{iso}} = -946$ ppm, $\delta_\delta = 135$ ppm, $\eta_\delta = 0.3$, $C_Q = 11.5$ MHz, $\eta_Q = 0.1$, $\alpha, \beta, \gamma = 0, 0, 0$. (3) Simulated spectrum using GIPAW calculated parameters for the optimized structure (see text), $\delta_{\text{iso}} = -893$ ppm, $\delta_\delta = 125$ ppm, $\eta_\delta = 0.0$, $C_Q = -16.1$ MHz, $\eta_Q = 0.0$, $\alpha, \beta, \gamma = 79, 0, 76$.

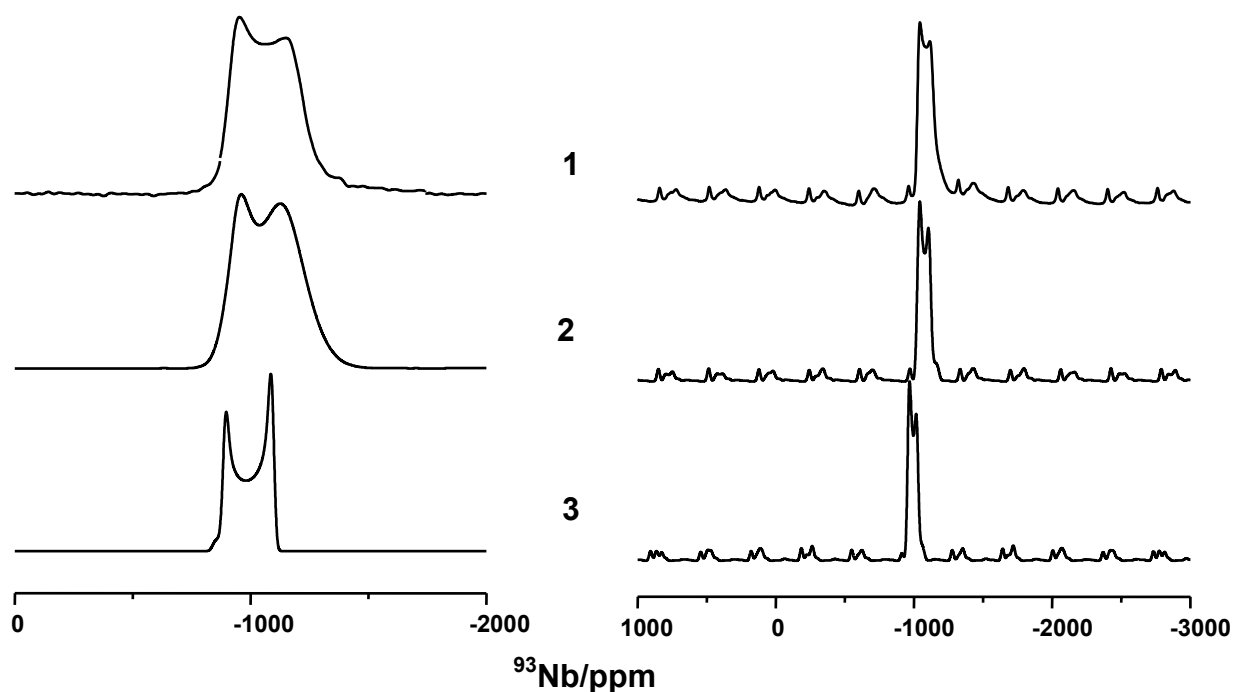


Figure S4. ^{93}Nb NMR spectra of LiNbO_3 (I) ($\text{Li}_{0.938}\text{Nb}_{0.012}\text{NbO}_3$) at 9.4 T acquired under stationary conditions (left) and under 30 kHz MAS (right). (1) Experimental spectra. (2) Simulated spectra based on experimental data, $\delta_{\text{iso}} = -1005 \text{ ppm}$, $\delta_\delta = 75 \text{ ppm}$, $\eta_\delta = 0.007$, $C_Q = 21.5 \text{ MHz}$, $\eta_Q = 0.0$, $\alpha, \beta, \gamma = 126, 0, 85$, Gaussian distribution of C_Q with 3 MHz width. (3) Simulated spectra using NMR parameters obtained by GIPAW for LiNbO_3 (I), $\delta_{\text{iso}} = -940 \text{ ppm}$, $\delta_\delta = 101 \text{ ppm}$, $\eta_\delta = 0.007$, $C_Q = 19.34 \text{ MHz}$, $\eta_Q = 0.0$, $\alpha, \beta, \gamma = 126, 0, 85$.

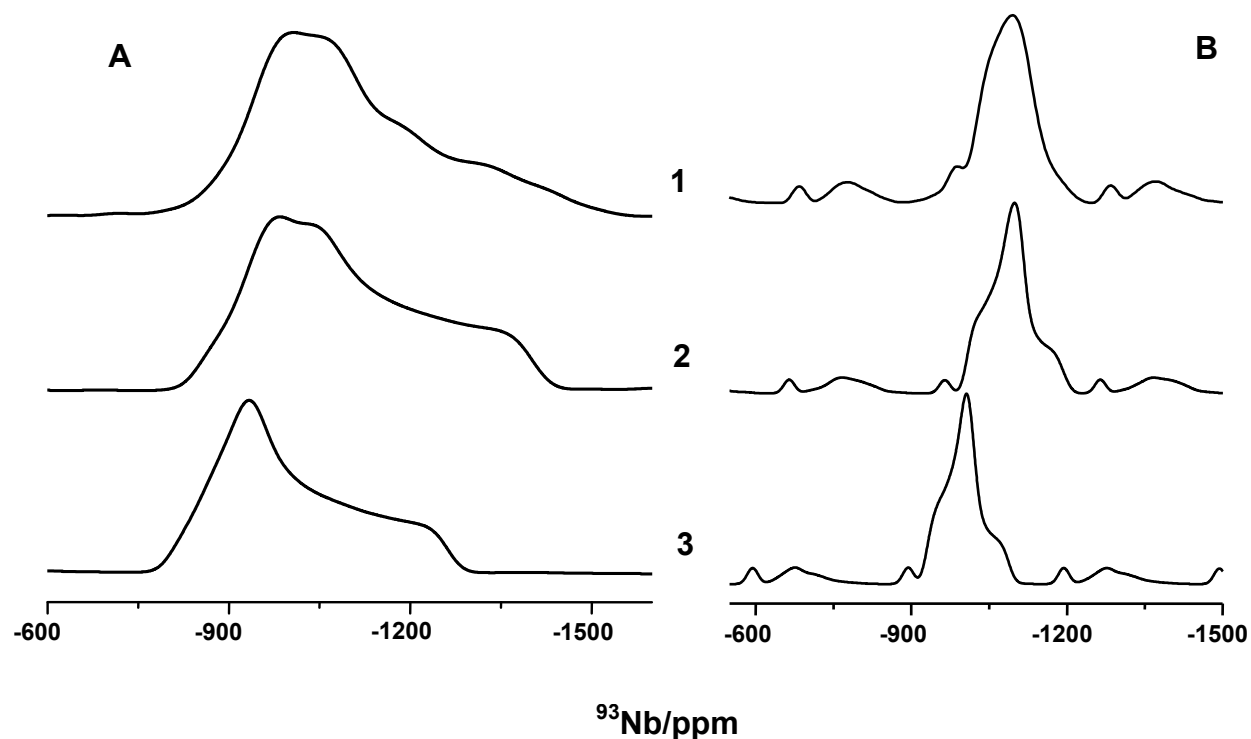


Figure S5. ^{93}Nb NMR spectra of KNbO_3 at 9.4 T acquired under stationary conditions in (A) and under 29 kHz MAS in (B). (1) Experimental spectra. (2) Simulated spectra using NMR parameters determined in this work from the experimental spectra, $\delta_{\text{iso}} = -1007$ ppm, $\delta_{\delta} = -60$ ppm, $\eta_{\delta} = 0.30$, $C_Q = 22.00$ MHz, $\eta_Q = 0.82$, $\alpha, \beta, \gamma = 20, 90, 90$. (3) Simulated spectra with NMR parameters obtained via GIPAW calculations, $\delta_{\text{iso}} = -935$ ppm, $\delta_{\delta} = -60$ ppm, $\eta_{\delta} = 0.743$, $C_Q = -21.56$ MHz, $\eta_Q = 0.96$, $\alpha, \beta, \gamma = 114, 90, 90$.

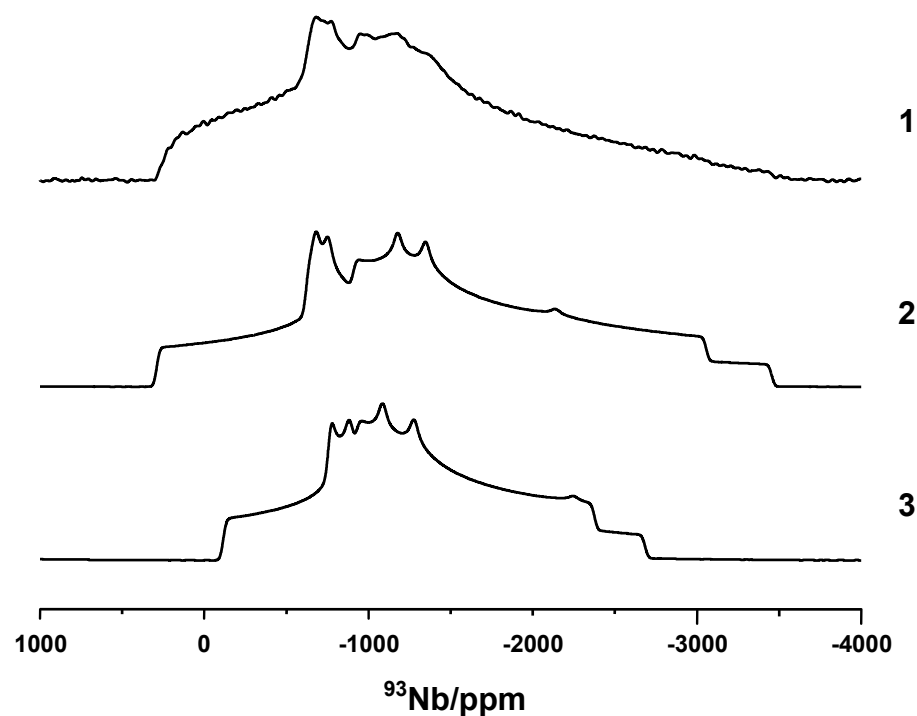


Figure S6. ^{93}Nb NMR spectra of a stationary powdered sample of CaNb_2O_6 acquired at 9.4 T. (1) Experimental spectrum. (2) Simulated spectrum with NMR parameters determined in [2] based on the experimental spectra, $\delta_{\text{iso}} = -975 \text{ ppm}$, $\delta_{\delta} = -291 \text{ ppm}$, $\eta_{\delta} = 0.619$, $C_Q = 50.40 \text{ MHz}$, $\eta_Q = 0.787$, $\alpha, \beta, \gamma = 43, 37, 10$. (3) Simulated spectrum with NMR parameters obtained by GIPAW, $\delta_{\text{iso}} = -988 \text{ ppm}$, $\delta_{\delta} = -258 \text{ ppm}$, $\eta_{\delta} = 0.331$, $C_Q = -41.49 \text{ MHz}$, $\eta_Q = 0.77$, $\alpha, \beta, \gamma = 61, 45, 27$.

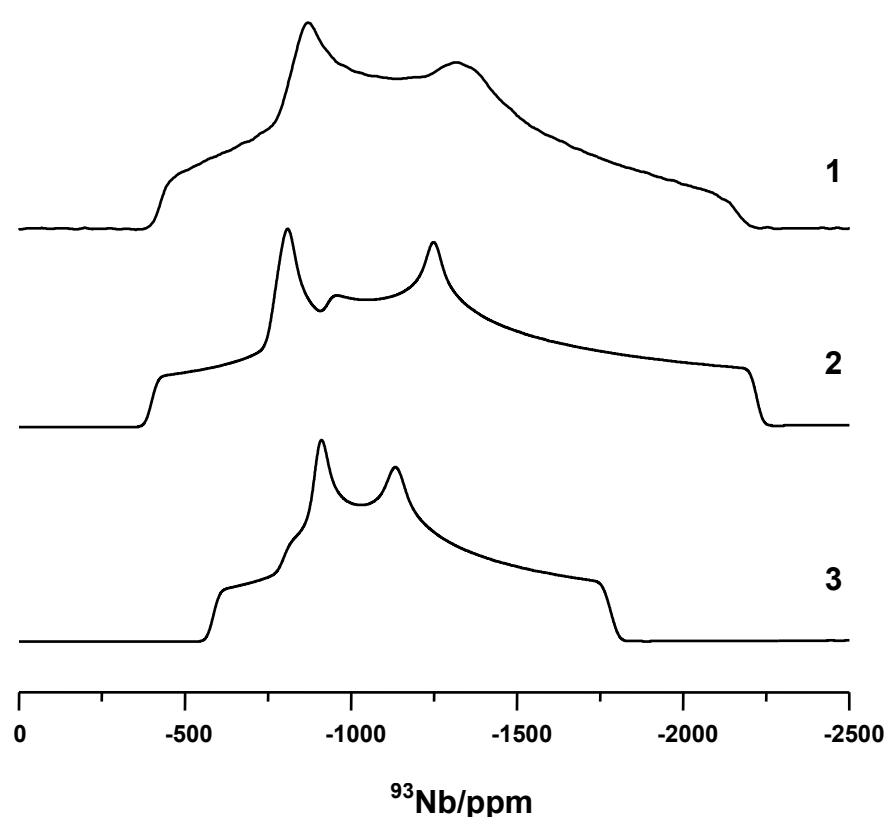


Figure S7. ^{93}Nb NMR spectra of a stationary powdered sample of SnNb_2O_6 acquired at 9.4 T. (1) Experimental spectrum. (2) Simulated spectrum using NMR parameters reported in [1] based on the experimental spectra, $\delta_{\text{iso}} = -1010 \text{ ppm}$, $\delta_{\delta} = 0.0 \text{ ppm}$, $\eta_{\delta} = 0.0$, $C_Q = 40 \text{ MHz}$, $\eta_Q = 0.45$, $\alpha, \beta, \gamma = 0, 0, 0$. (3) Simulated spectrum using NMR parameters obtained by GIPAW, $\delta_{\text{iso}} = -978 \text{ ppm}$, $\delta_{\delta} = 141 \text{ ppm}$, $\eta_{\delta} = 0.693$, $C_Q = -32.86 \text{ MHz}$, $\eta_Q = 0.56$, $\alpha, \beta, \gamma = 124, 4, 53$.

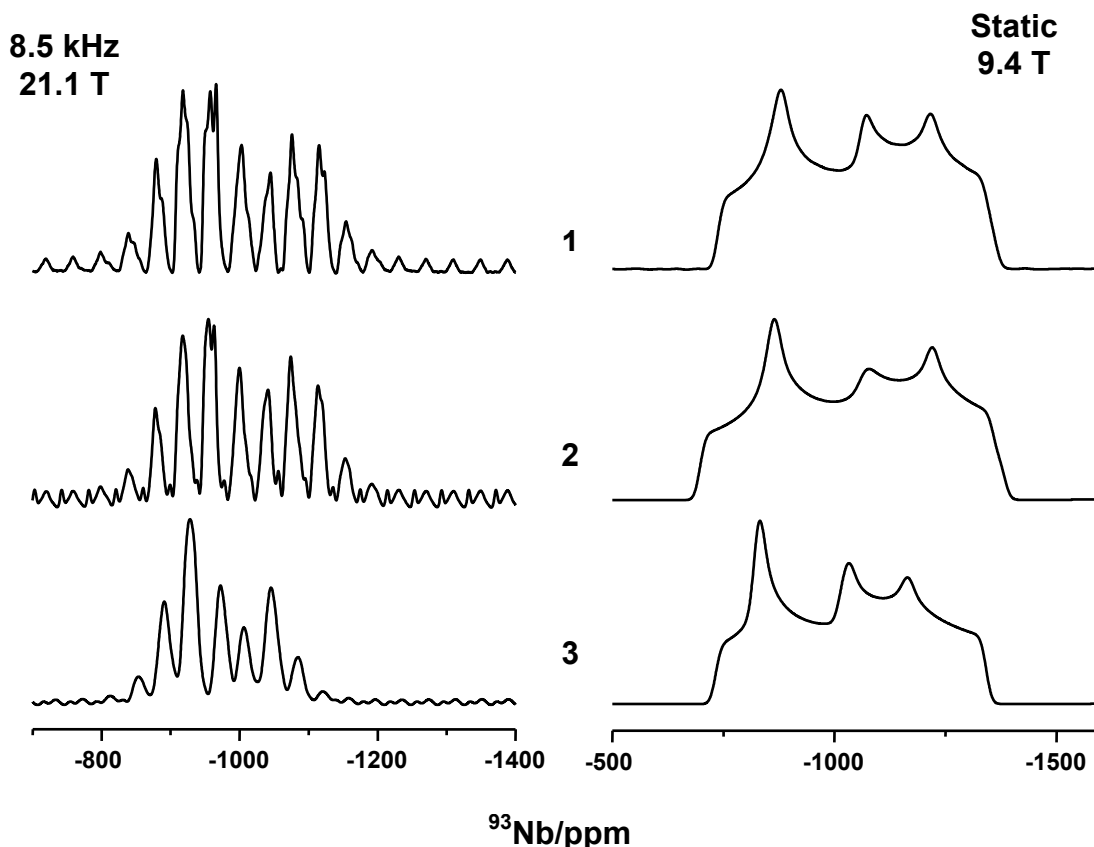


Figure S8. 8.5 kHz MAS and stationary ^{93}Nb NMR spectra of BiNbO_4 acquired at 21.1 T and 9.4 T as indicated. (1) Experimental spectra. (2) Simulated spectra with NMR parameters determined in this work from the experimental spectra, $\delta_{\text{iso}} = -977$ ppm, $\delta_{\delta} = -150$ ppm, $\eta_{\delta} = 0.560$, $C_Q = 20.70$ MHz, $\eta_Q = 0.51$, $\alpha, \beta, \gamma = 24, 22, 78$. (3) Simulated spectra using NMR parameters obtained by GIPAW based on the crystal structure, $\delta_{\text{iso}} = -955$ ppm, $\delta_{\delta} = -118$ ppm, $\eta_{\delta} = 0.177$, $C_Q = -21.76$ MHz, $\eta_Q = 0.56$, $\alpha, \beta, \gamma = 0.25, 90$.

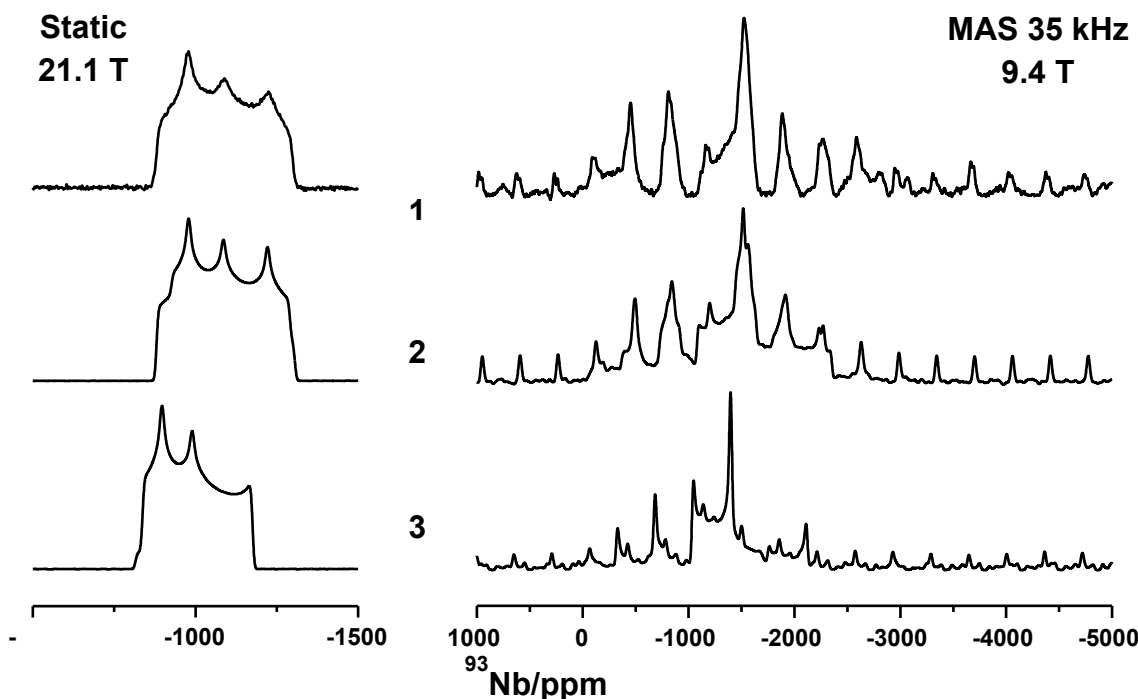


Figure S9. ^{93}Nb NMR spectra of a powdered sample of La_3NbO_7 acquired at 21.1 T (left) and 9.4 (right, MAS 35 kHz). (1) Experimental spectrum. (2) Simulated spectrum based on experimental NMR parameters determined in this work, $\delta_{\text{iso}} = -1015 \text{ ppm}$, $\delta_\delta = 113 \text{ ppm}$, $\eta_\delta = 0.69$, $C_Q = 49 \text{ MHz}$, $\eta_Q = 0.275$, $\alpha, \beta, \gamma = 50, 27, 72$. (3) Simulated spectrum using NMR parameters obtained by GIPAW calculations, $\delta_{\text{iso}} = -930 \text{ ppm}$, $\delta_\delta = 153 \text{ ppm}$, $\eta_\delta = 0.023$, $C_Q = -45.52 \text{ MHz}$, $\eta_Q = 0.027$, $\alpha, \beta, \gamma = 90, 19, 0$.

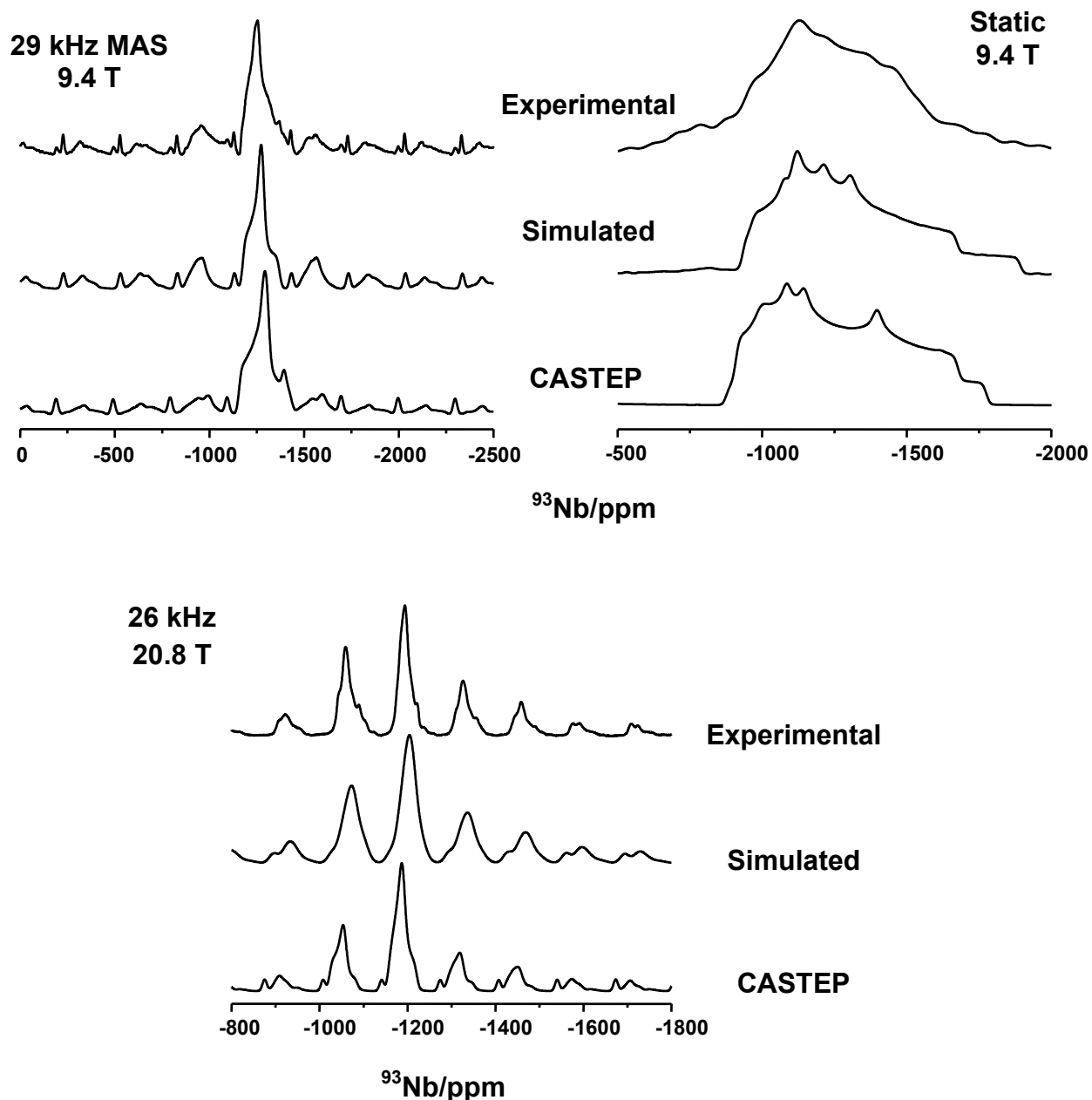


Figure S10. ^{93}Nb NMR $\text{Te}_3\text{Nb}_2\text{O}_{11}$ acquired at 9.4 T (above) and at 20.8 T (below). Static and MAS NMR spectra are shown as indicated. (**Upper traces**) Experimental spectra. (**Middle traces**) Simulated spectra using experimental NMR parameters determined in this work, $\delta_{\text{iso}} = -1176$ ppm, $\delta_{\delta} = -320$ ppm, $\eta_{\delta} = 0.680$, $C_Q = 26.00$ MHz, $\eta_Q = 0.97$, $\alpha, \beta, \gamma = 166, 70, 51$. (**Lower traces**) Simulated spectra based on GIPAW-calculated NMR parameters, $\delta_{\text{iso}} = -1156$ ppm, $\delta_{\delta} = -306$ ppm, $\eta_{\delta} = 0.256$, $C_Q = -26.29$ MHz, $\eta_Q = 0.89$, $\alpha, \beta, \gamma = 172, 85, 50$.

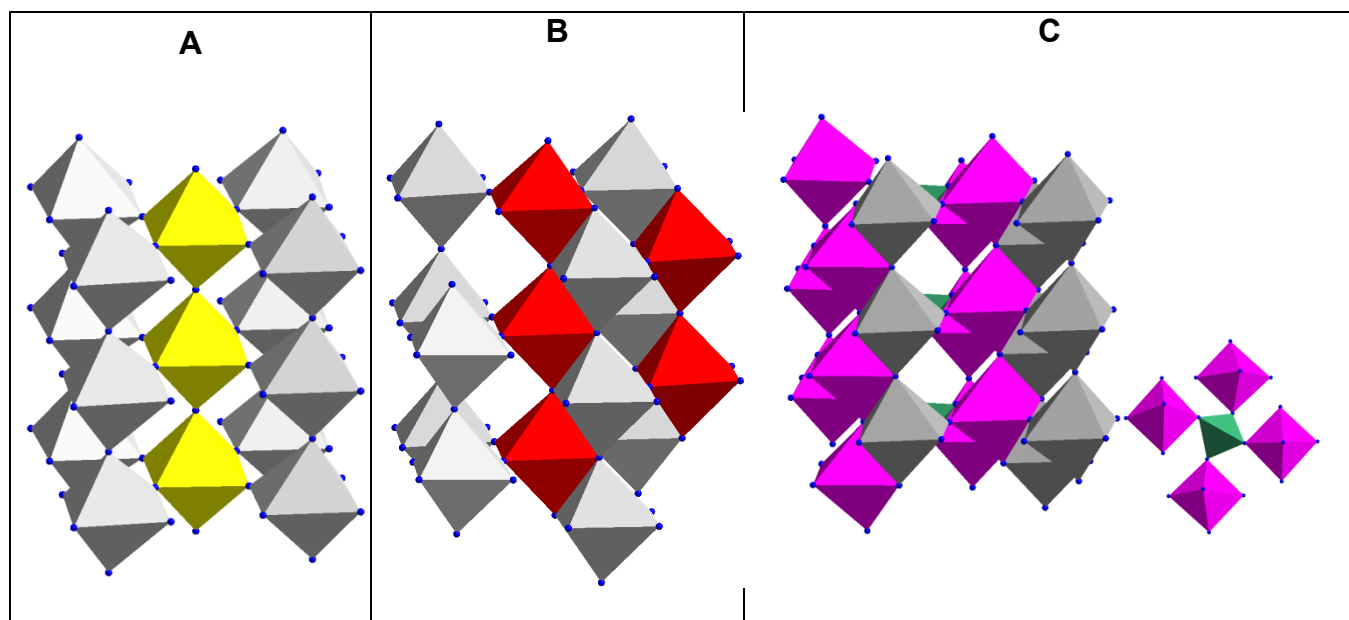


Figure S1. Polyhedral representation of the crystal structure of VNb₉O₂₅. **(Panel A)** Nb1 octahedra in yellow are shown connected to Nb2 octahedra in gray. **(Panel B)** Nb2 octahedra in red are shown connected to Nb3 and Nb1 octahedra in gray. **(Panel C)** Nb3 octahedra in pink are shown connected to Nb2 octahedra in gray and to VO₄ tetrahedra in green. Inset on the right shows that each VO₄ tetrahedron (green) is connected only to Nb3 octahedra (pink).

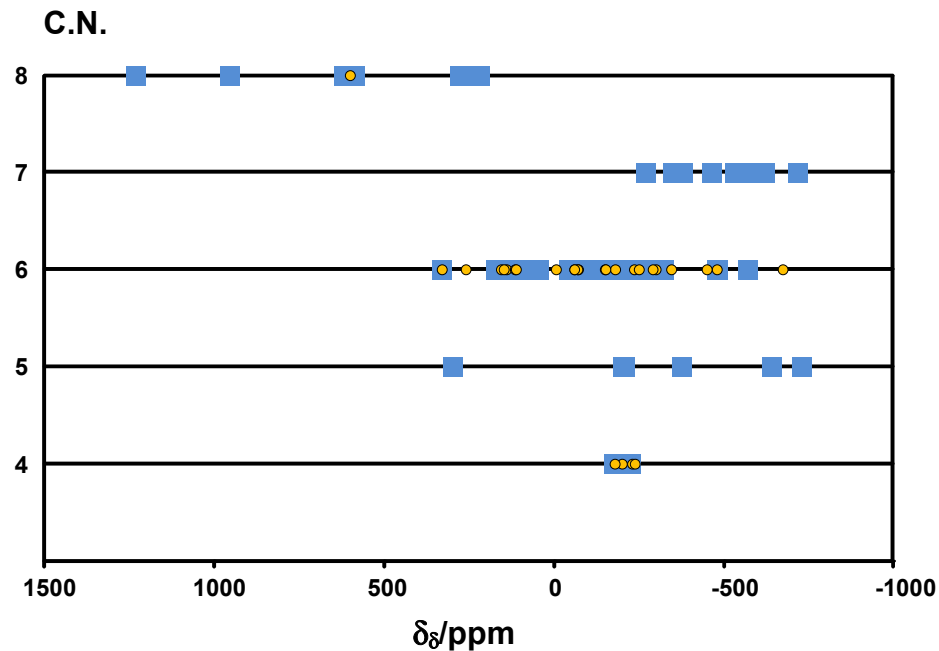


Figure S12. Anisotropy of ^{93}Nb chemical shielding in niobates, $\delta_{\delta}(^{93}\text{Nb})$, as a function of NbO_x coordination number (C.N.). GIPAW-calculated theoretical values are shown as blue squares, while the experimentally determined anisotropy values are shown as yellow circles.

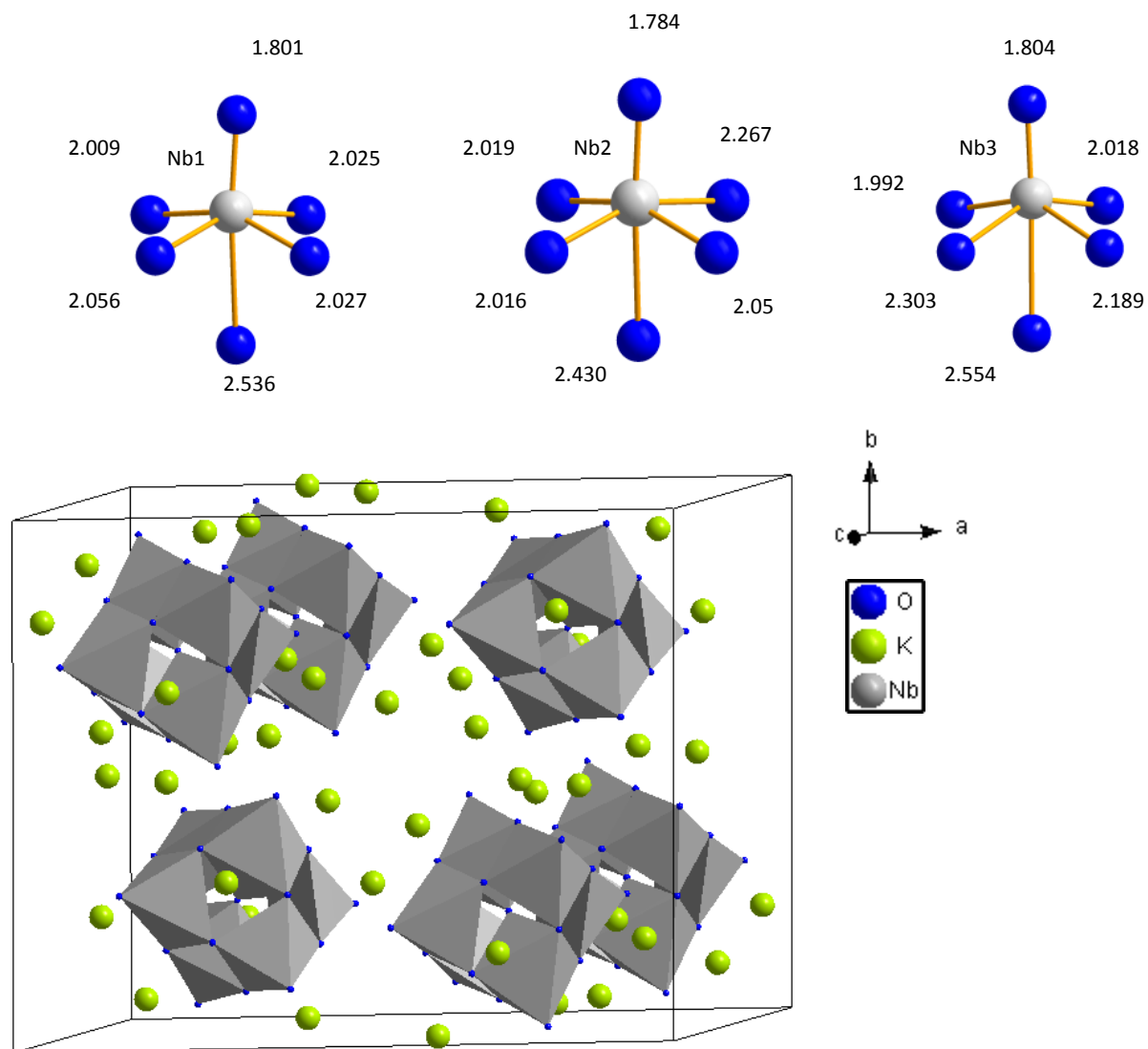


Figure S2. Optimized crystal structure of $\text{K}_8\text{Nb}_6\text{O}_{19}$ (below) and the coordination oxygen environment of the three non-equivalent niobium sites in this crystal structure (above).

References

1. Lapina, O.B., et al., *Practical aspects of ^{51}V and ^{93}Nb solid-state NMR spectroscopy and applications to oxide materials.* Prog. Nucl. Magn. Reson. Spectrosc., 2008. **53**(3): p. 128-191.
2. Hanna, J.V., et al., *A Nb-93 Solid-State NMR and Density Functional Theory Study of Four- and Six-Coordinate Niobate Systems.* Chemistry-a European Journal, 2010. **16**(10): p. 3222-3239.